Carbohydrate Polymers 83 (2011) 144–150

Contents lists available at ScienceDirect

Carbohydrate Polymers

journal homepage: www.elsevier.com/locate/carbpol

Preparation and characterization of antimicrobial chitosan-*N*-arginine with different degrees of substitution

Bo Xiao, Ying Wan, Maoqi Zhao, Yiqun Liu, Shengmin Zhang*

Advanced Biomaterials and Tissue Engineering Center, Huazhong University of Science and Technology, Wuhan 430074, PR China

ARTICLE INFO

Article history:
Received 5 March 2010
Received in revised form 7 June 2010
Accepted 16 July 2010
Available online 24 July 2010

Keywords:
Chitosan-*N*-arginine
Degree of substitution
Antimicrobial activity

ABSTRACT

A series of water-soluble chitosan-*N*-arginine (CS-*N*-Arg) with various degrees of substitution (DSs) from 8.7 to 28.4% was synthesized by reacting amino groups of chitosan with arginine. The chemical structures and physical properties of CS-*N*-Arg were characterized by Fourier-transform infrared, magnetic resonance spectra, elemental analysis and X-ray diffraction as well as thermogravimetric analysis. Results showed that CS-*N*-Arg had a more amorphous structure than that of chitosan, and the thermal stability of CS-*N*-Arg was slightly lower than that of chitosan. It was found that CS-*N*-Arg samples were able to inhibit almost all the bacteria (*Staphylococcus aureus* and *Escherichia coli*) at a concentration higher than 150 ppm, whereas they could promote the growth of bacteria at a concentration lower than 50 ppm. The antibacterial activity of CS-*N*-Arg samples was dependent on both DS and concentrations changed in the range from 50 to 150 ppm. Due to their enhanced antimicrobial properties, CS-*N*-Arg materials would be promising candidates for the applications in skin tissue engineering.

1. Introduction

Chitosan is a deacetylated derivative of chitin, which is the second most abundant natural polysaccharide after cellulose (Arvanitoyannis, 1999). Antibacterial activity of chitosan has been considered as one of its interesting properties (Chiang, Wang, & Lee, 2009). So far, it is basically clear that the antibacterial functions of chitosan are arisen from its positively charged properties (Gil, del Mónaco, Cerrutti, & Galvagno, 2004). In principle, chitosan can kill some kinds of microbes by disrupting their normal structure due to the reactions between the positive charges of chitosan and the negatively charged cell walls of bacteria or proteins inside (Holappa et al., 2006). However, the antibacterial functions of chitosan are limited because amino groups on chitosan backbone can only function as relatively weak positive charge centers. To improve the antimicrobial activity of chitosan, it is reasonable to enhance the strength of positive charges on the chitosan molecules by endowing it with some more positively charged groups. Many efforts, therefore, have been made to synthesize some new antimicrobial chitosan derivatives such as acyl thiourea derivatives of chitosan, *N*-trimethyl chitosan, *N*-diethyl methyl chitosan and chitosan-*N*-2-hydroxypropyl trimethyl ammonium chloride (Qin et al., 2004; Sadeghi et al., 2008; Zhong et al., 2008).

Guanidine is one of strong organic bases in considering its dissociation constant ($pK_a = 13.6$) (Gobbi & Frenking, 1993). In general, the positive electronic strength of the groups in organic bases is ranked in the following way: guanidine group > quaternary group > alkylamino group > aromatic amine (Yao, 1994). Since guanidine group seems to show the strongest positive electricity and it is positively charged in acidic, neutral and basic solutions, guanidine derivatives, therefore, have been investigated as antibacterial and antivirus materials (Baker, Luedtke, Tor, & Goodman, 2000; El-Azzami & Grulke, 2009; Zhang, Jiang, & Chen, 1999). Some guanidine-contained polymers can function as polyelectrolytes and are capable of being against some Gram-positive or -negative bacteria even though they sometimes show low mammalian toxicity (Guan, Xiao, Sullivan, & Zheng, 2007). Several reports have indicated that chitosan-*N*-arginine (CS-*N*-Arg) has desirable biocompatibility, high gene transfection efficiency and good anticoagulation activity (Liu, Zhang, Cao, Xu, & Yao, 2004; Zhu et al., 2007). In view of the functions of guanidine, CS-*N*-Arg could be expected to show enhanced antibacterial activities than that of chitosan and serve as a desirable material for antimicrobial applications.

Materials for skin tissue engineering need to meet some specific requirements for the antibacterial applications due to the common infection in clinic treatment. The object of this study is to synthesize a series of CS-*N*-Arg samples with various DSs and investigate their antimicrobial activities against *Staphylococcus aureus* and *Escherichia coli*, and screen desirable materials for skin tissue engineering.

* Corresponding author at: Advanced Biomaterials and Tissue Engineering Center, Huazhong University of Science and Technology, Life Science Building, 1037 Luoyu Rd, Wuhan 430074, PR China. Tel.: +86 27 8779 2216; fax: +86 27 8779 2205.
E-mail address: smzhang@mail.hust.edu.cn (S. Zhang).

0144-8617/$ – see front matter © 2010 Elsevier Ltd. All rights reserved.
doi:10.1016/j.carbpol.2010.07.032

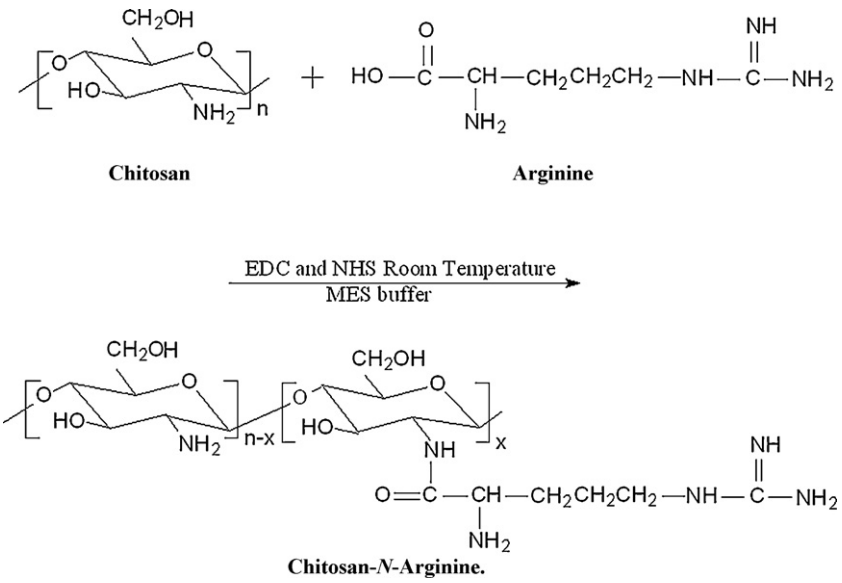

Fig. 1. Synthetic scheme of chitosan-*N*-arginine (CS-*N*-Arg) using EDC and NHS as catalysts in MES buffer at room temperature.

2. Materials and methods

2.1. Materials

Chitin was purchased from Aldrich. Chitosan was obtained by highly deacetylating chitin following a known method (Mima, Miya, Iwamoto, & Yoshikawa, 2003). 2-(*N*-morpholino) ethanesulfonic acid sodium salt (MES) was purchased from Amresco Commercial Finance, Inc. Peptone was obtained from Shanghai Regal Biotech Technology, Inc (China). 1-Ethyl-3-(3-dimethylaminopropyl) carbodiimide hydrochloride (EDC) and *N*-hydroxysulfosuccinimide sodium salt (NHS) were purchased from Shanghai Huishen Chemical Co., Ltd. (China). L-Arginine, beef extract and agar were supplied by Sinopharm Chemical Reagent Co., Ltd. (China). Other chemicals were of analytical grade. *S. aureus* (CCTCC AB910393) and *E. coli* (CCTCC AB91112) were supplied by the Chinese Center of Type Culture Collection, Wuhan University, China.

2.2. Depolymerization and intrinsic viscosity measurement

Molecular weight of chitosan samples obtained above was tailored by depolymerization using sodium nitrite following a reported method (Lavertu, Méthot, Tran-Khanh, & Buschmann, 2006). Viscosity-average molecular weight of the resultant chitosan was determined as 5.2×10^4 using a 0.5 M CH_3COOH/0.2 M CH_3COONa solvent system (Badawy & Rabea, 2009).

2.3. Synthesis of chitosan-N-arginine

The CS-*N*-Arg samples were synthesized by a modified method described in some reports and synthetic scheme is given in Fig. 1 (Chung et al., 2002; Liu, Zhang, et al., 2004). 3 g of chitosan was dissolved in 600 mL of MES buffer (25 mM, pH 5.0). The carboxyl group of arginine was activated for 2 h by NHS/EDC in MES buffer. At a fixed molar ratio of EDC/NHS/arginine of 4:4:1, several mixtures were prepared by adding the activated arginine solution into the chitosan solution, and resultant mixtures were allowed to react at ambient temperature with stirring for 12, 24 and 48 h, respectively. The reactions were quenched by adding hydroxylamine, and adjusting pH of reaction systems to 8.0 with addition of a NaOH solution. The collected products were dialyzed (MWCO = 3500) against distilled water for 4 days and lyophilized. The final products were named as CS-*N*-Arg-1, CS-*N*-Arg-2 and CS-*N*-Arg-3, respectively, and the DSs of arginine were denoted by the numbers followed Arg.

2.4. Characterization

Infrared spectra of chitosan and CS-*N*-Arg samples were measured using a Bruker EQUINOX 55 FT-IR spectrophotometer. Powder samples were mixed with KBr, and the mixtures were pressed into disks for measurements.

^{13}C NMR spectrum was recorded on a Bruker Avance spectrometer (INOVA-400 NMR). 150 mg of CS-*N*-Arg-3 was dissolved in 15 mL of 0.1 M HCl solution with stirring overnight, and 3 mL of 1.5 wt% $NaNO_2$ solution was added to further decrease the molecular weight of CS-*N*-Arg-3 (An, Thien, Dong, & Dung, 2009). The obtained products were filtrated through a micro-filter and lyophilized. After that, the resultant CS-*N*-Arg-3 was dissolved in D_2O to prepare a 30 wt% solution for NMR measurements.

DS of CS-*N*-Arg was determined by elemental analysis (C, N) using a Vario Micro cube elemental analysis instrument (Elementar Co., German).

XRD patterns of the samples were recorded on an X-ray diffractometer (X'Pert PRO, PANalytical B.V. Holland) at a voltage of 40 kV and a current of 40 mA using CuKa radiation. The scanning scope of 2θ was ranged from 5° to 40° at ambient temperature (Arvanitoyannis, Kolokuris, Nakayama, Yamamoto, & Aiba, 1997).

The water-solubility of chitosan and its derivatives was estimated at room temperature using turbidity measurement (Jintapattanakit, Mao, Kissel, & Junyaprasert, 2008). The dry sample (30 mg) was dissolved in 50 mL of 0.1 M HCl solution for 3 h with constant stirring with addition of 0.1 or 1.0 M NaOH solution stepwise, the transmittance of the solution was recorded on a PuXi TU-1810 UV–visible spectrophotometer (China) and data were collected at 600 nm.

Thermal degradation of samples was monitored using a thermal analyzer (PerkinElmer Instruments Pyris 1 TGA). The samples were heated from ambient temperature to 600 °C at a constant heating rate of 10 °C/min under a nitrogen atmosphere.

Table 1
Elemental analysis results of different samples.

Samples	C (%)	N (%)	Reaction time (h)	DD (%)	DS (%)
Chitosan	38.55 ± 0.08	6.993 ± 0.05	–	78.4	–
CS-*N*-Arg-1	42.51 ± 0.04	10.91 ± 0.01	12	–	8.7
CS-*N*-Arg-2	42.93 ± 0.02	14.08 ± 0.01	24	–	18.1
CS-*N*-Arg-3	44.30 ± 0.05	16.94 ± 0.03	48	–	28.4

DD is the degree of deacetylation; DS is the degree of substitution.

2.5. Antimicrobial tests

The antimicrobial activities of chitosan and CS-*N*-Arg samples were determined by a plate count agar (PCA) method. Strains of *S. aureus* and *E. coli* were cultured on nutrient agar slope (peptone 1%, NaCl 0.5%, beef extract 0.3%, agar 2%, pH 7.2–7.4). Suspensions were prepared by transferring sterile 0.9% saline to the slope. Then 10-fold dilutions were made to get a final concentration of 600 cells/mL for the antibacterial test. Prior to experiments, an acetic acid (HAc) solution was prepared and used as a reference. Chitosan and CS-*N*-Arg samples were respectively dissolved in a 0.3 (v/v) % HAc solution to prepare 0.5 wt% solutions, and these solutions were micro-filtrated through a syringe filter. Then, the solution was added to the beef extract–peptone medium to produce different mixtures with various concentrations: 50, 100, 150, 200, 300, 400, and 500 ppm. These mixtures were shaken gently to disperse HAc, chitosan, CS-*N*-Arg throughout the agar plates. Afterwards, 0.4 mL of diluted bacteria solution was spread onto agar plates. After incubation at 37 °C for 24 h, the number of colonies was counted to measure the antibacterial activity. Survival percentage was defined as follows (Kitagaki, Araki, Funato, & Shimoi, 2007; Lu et al., 2008):

$$\text{survival \%} = \frac{\text{colony numbers of treated bacteria}}{\text{colony numbers of control bacteria}} \times 100$$

3. Results and discussion

3.1. Preparation of chitosan-N-arginine samples

During the process of guanidination, EDC was reacted with the carboxyl groups of arginine to form the amine-reactive *O*-acylisourea intermediate (Chung et al., 2002). However, the intermediate is susceptible to hydrolysis, making it short-lived in aqueous solution. Then the addition of NHS stabilizes the unstable amine-reactive intermediate by converting it to the semistable amine-reactive NHS ester, thus increasing the efficiency of EDC-mediated coupling reaction. Finally, the activated carboxylic groups of arginine form stable amido links through the reaction of amino groups of chitosan. The reaction conditions for guanidination of chitosan are summarized in Table 1. Under present reaction conditions, by fixing the ratio of arginine to chitosan as constant and selecting an optimized amount of catalyst, DSs of CS-*N*-Arg seem to proportionally increase with reaction time. Results shown in Table 1 may suggest that DSs of CS-*N*-Arg could be feasibly controlled by the reaction time.

3.2. Characterization of chitosan-N-arginine samples

The IR spectra of chitosan and CS-*N*-Arg samples are shown in Fig. 2. The broad band at around 3450 cm^{-1} is attributed to –NH, –OH stretching vibration and inter- and extra-molecular hydrogen bond of chitosan molecules. The weak band at 2921 cm^{-1} is ascribed to –CH– stretch of chitosan. The characteristic peaks at 1650 and 1600 cm^{-1} are corresponded to the C=O stretch of the amide I and $-NH_2$ bands of chitosan, respectively. The peaks matched with saccharide backbone are easily viewed at 1158 cm^{-1} (anti-symmetric stretching of the C–O–C), and 1086–1020 cm^{-1} (skeletal vibrations involving the C–O stretching). In comparison to chitosan, several noticeable changes occur in the spectra of CS-*N*-Arg samples. The characteristic band of guanido group at around 1630 cm^{-1} is observed, indicating that arginine has been already successfully coupled to chitosan. The new band at around 1520 cm^{-1} is most likely due to an amide bond linking chitosan and arginine (Liu, Zhang, et al., 2004). In addition, it can be seen that the peak at 1600 cm^{-1} for primary amine $-NH_2$ bending disappears in CS-*N*-Arg owing to the introduction of arginine.

To obtain a CS-*N*-Arg-3 solution with a high concentration, further depolymerization of CS-*N*-Arg-3 has been done. In mildly acidic solutions at room temperature, in general, nitrosating species can attack the amine groups of chitosan, and subsequently cleave the β-glycosidic linkages of chitosan, resulting in 2,5-anhydro-D-mannose units at the reducing end of the cleaved polymer (Allan & Peyron, 1995). Fig. 3 presents ^{13}C NMR spectrum of so-produced CS-*N*-Arg-3. The main peaks are basically in agreement with reported results (Liu, Zhang, et al., 2004). Some non-typical peaks in the spectrum can be ascribed the effect of depolymerization, which was also observed by other researchers (Kumirska et al., 2009). In addition, spectrum of the anomeric carbon is quite weak and it is also possibly resulted from depolymerization of the sample. Fig. 3 confirms that there exist methylene (43.0 ppm) and guanido (170.2 ppm) bands in CS-*N*-Arg, further suggesting that CS-*N*-Arg has been already successfully synthesized.

To make a comparison of crystalline properties among different samples, some representative X-ray patterns are provided in Fig. 4. It is observed that the diffractogram of unmodified chitosan shows two characteristic diffractive peaks located at around 10.7° and 19.9°, indicating the high degree of crystallinity of chitosan similar to the reported results (Zhang, Xue, Xue, Gao, & Zhang,

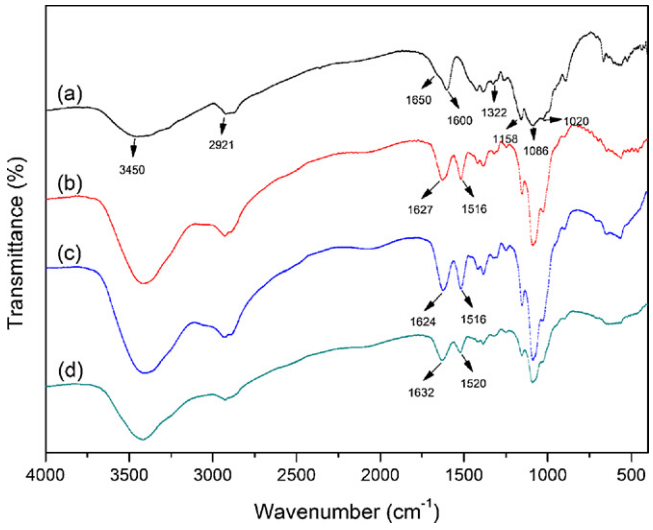

Fig. 2. FT-IR spectra of chitosan (a) and chitosan-*N*-arginine (CS-*N*-Arg) samples with various degrees of substitution: 8.7% (b); 18.1% (c) and 28.4% (d). The description of chitosan and CS-*N*-Arg samples is given in Table 1.

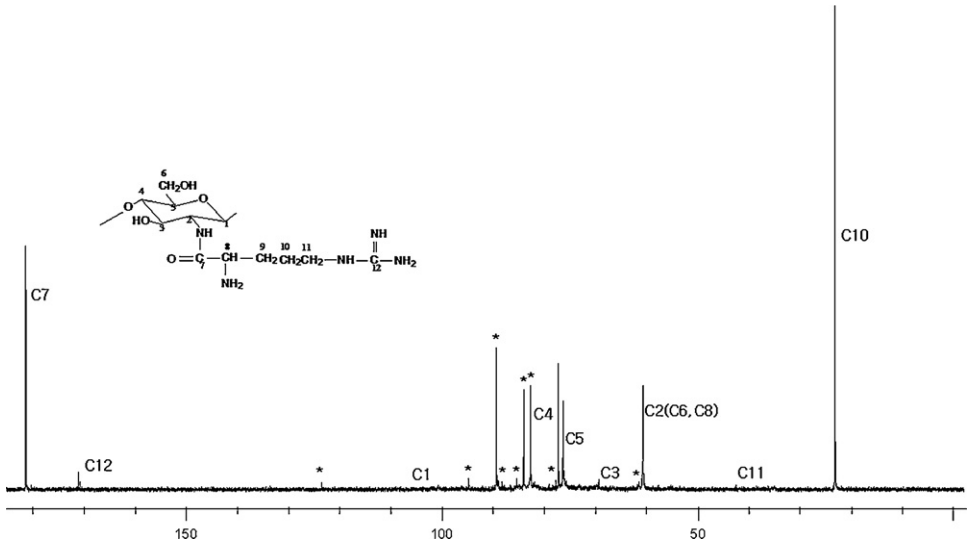

Fig. 3. ^{13}C NMR spectrum of depolymerized chitosan-*N*-arginine (DS = 28.4%) with nitrous acid. Artifact signals (*) are visible in the spectrum of the depolymerized sample besides the signals typical of CS-*N*-Arg.

2005). In comparison to unmodified chitosan, the X-ray patterns of CS-*N*-Arg samples exhibit some changes in both its diffraction angles and peak intensity. In the spectrum of the CS-*N*-Arg samples, a peak originally recorded at 10.7° for chitosan is shifted to a higher 2θ value of around 12.5°, and another peak for chitosan component at 29.9° almost disappears. In addition, it can be seen that there are no significant differences observed for different CS-*N*-Arg samples with various DSs. The lower crystallinity of CS-*N*-Arg can be ascribed to the presence of arginine side chains which will certainly hinder the formation of inter- and extra-molecular hydrogen bonds. As a result, CS-*N*-Arg samples are expected to show significantly decreased crystallinity compared to the unmodified chitosan.

The pH-dependent solubilities of chitosan and CS-*N*-Arg samples are shown in Fig. 5. All samples show good solubilities at pH < 7. It is clear that chitosan can be dissolved in a dilute acidic solution due to the protonation of the amino groups. With respect to CS-*N*-Arg samples, the introduction of arginine to chitosan main chains reduces the hydrogen bond interactions and makes the samples soluble in the medium. In the pH ranging from 7 to 7.5, the transmittance of the solutions of all samples is abruptly decreased since the samples are liable to transfer to flocky precipitate, as indicated in a report (Qin et al., 2004). When the pH of the solution is higher than 7.5, the turbidity reaches a plateau. It is known that a low protonation degree leads to low charge density and therefore small repulsive electrostatic force between its chains, resulting in formation of more hydrogen bonds and decreases in solubilities of the samples (Zhu et al., 2005), and as a result, all samples precipitate from the solutions. After being grafted with arginine, it might be difficult for CS-*N*-Arg samples to form orderly arranged crystalline structure through interactions between molecules. Consequently, the crystallinity of CS-*N*-Arg samples is significantly lower than that of chitosan (as shown in Fig. 4), and thus solubility of CS-*N*-Arg in neutral water is notably improved compared to that of unmodified chitosan.

TG curves of chitosan and CS-*N*-Arg samples are shown in Fig. 6(a). The thermogram of chitosan has two stages of weight loss. The first stage ranges between 30 and 150 °C and shows about 6.4% loss in weight, corresponding to the evaporation of adsorbed and bound water, together with the elimination of the possible

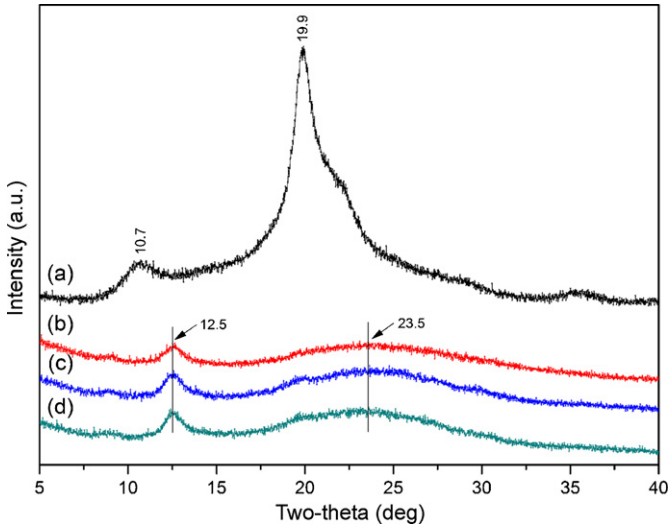

Fig. 4. XRD patterns of chitosan (a) and chitosan-*N*-arginine (CS-*N*-Arg) samples with various degrees of substitution: 8.7% (b); 18.1% (c) and 28.4% (d). The description of chitosan and CS-*N*-Arg samples is given in Table 1.

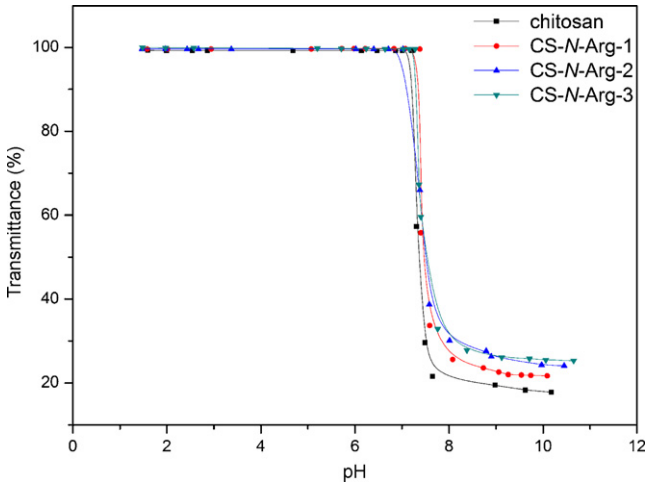

Fig. 5. pH-dependent of solubility of chitosan and chitosan-*N*-arginine (CS-*N*-Arg) samples with various degrees of substitution. The description of chitosan and CS-*N*-Arg samples is given in Table 1.

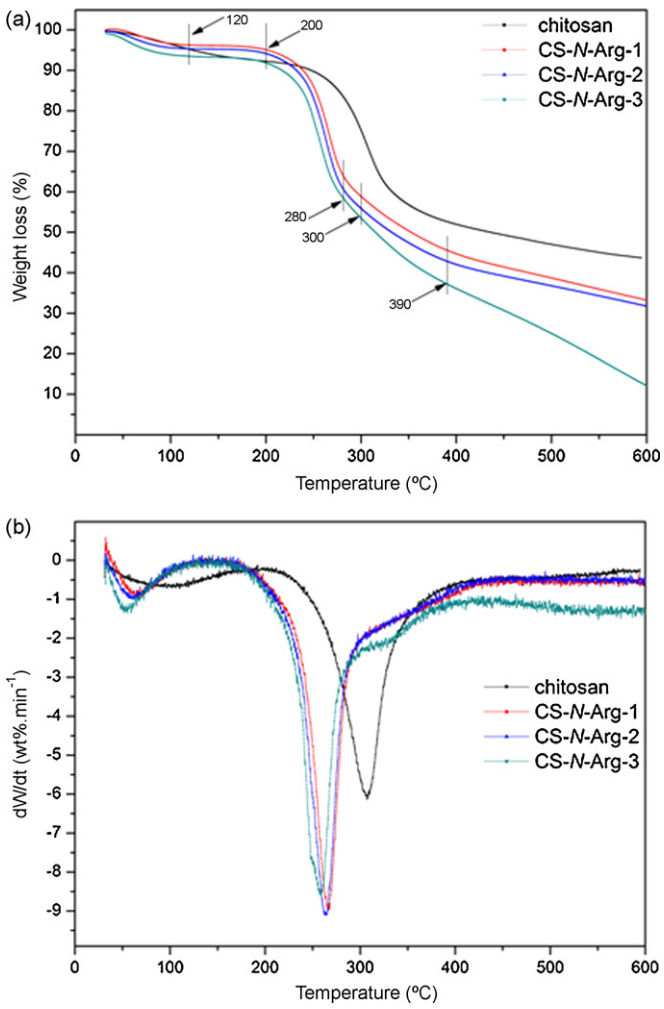

Fig. 6. TG (a) and DTG (b) of chitosan and chitosan-*N*-arginine (CS-*N*-Arg) samples with various degrees of substitution. The description of chitosan and CS-*N*-Arg samples is given in Tables 1 and 2.

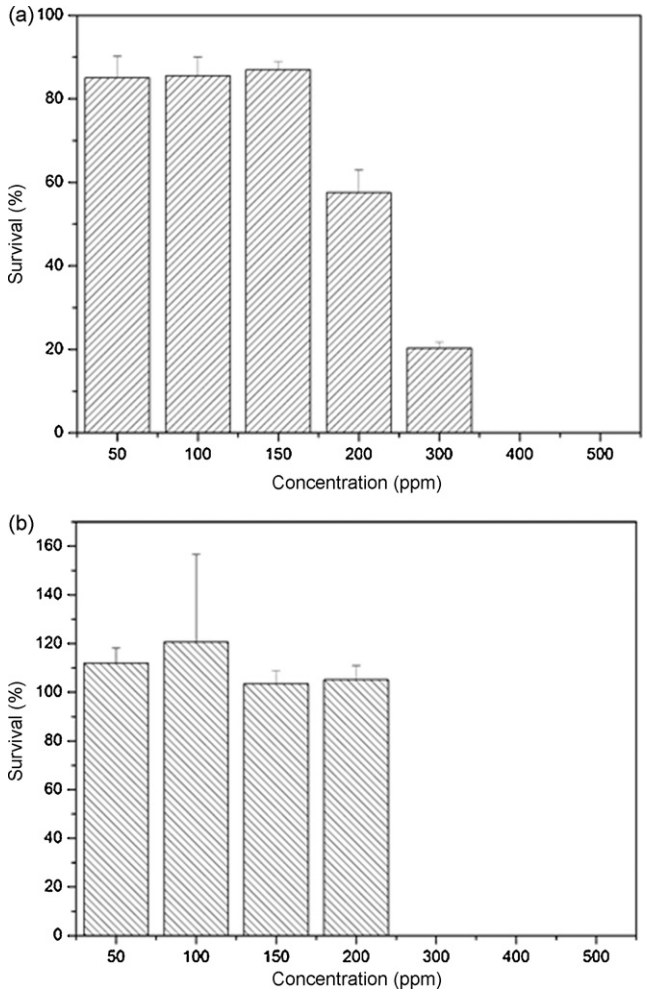

Fig. 7. Antibacterial activity of acetic acid (HAc) on *S. aureus* (a) and *E. coli* (b). *S. aureus* and *E. coli* cells were spread onto culture medium agar plates with different concentrations of HAc and incubated at 37 °C for 24 h. Data are mean ± standard deviation of quadruplicate.

trace amount of HAc. The second one starts at 230 °C and continues up to 400 °C during which there is 39.3% weight loss due to further dehydration of the saccharide rings, to deacetylation and degradation of chitosan. Comparing with chitosan, all the CS-*N*-Arg samples show a two-stage degradation behavior as well. The first stage occurs between 30 and 120 °C, associated with the loss of bound water in the samples. The second one, ranging from 200 to 280 °C, corresponds to further dehydration and degradation of the samples, together with the breakage of the amide linkage of CS-*N*-Arg. The curves shift to lower temperatures as the DS of the samples increasing from 8.7 to 28.4%.

To more quantitatively examine these plots, the weight-loss percents of all samples are differentiated, and collected data are depicted in Fig. 6(b) and also summarized in Table 2, respectively. The temperature value corresponding to the maximum degradation rate for different samples is marked with T_{max}. To make more detailed comparisons of the various thermal effects for four kinds of samples, the peaks at a lower or higher temperature are designated as T_{max1} and T_{max2}, respectively. Comparing with T_{max1} and weight loss of each sample, it can be seen that the adsorbed and bound water in CS-*N*-Arg samples is more easily evaporated than that of chitosan. In addition, water adsorbed in CS-*N*-Arg samples lose at various rates depending on the DSs of CS-*N*-Arg. Fig. 6(b) also shows that T_{max2} of chitosan is higher than that of CS-*N*-Arg, indicating that chitosan is more difficult to be discomposed in this phase. Additionally, CS-*N*-Arg samples with increased DS are more easily to be degraded.

3.3. Antimicrobial activity of HAc, chitosan and CS-N-Arg

3.3.1. Effect of concentrations on the antibacterial activity of HAc

Since HAc also has a certain antimicrobial activity, a series of blank (control) experiments was conducted to verify the results.

Fig. 7(a) illustrates the antimicrobial activity of HAc with different concentrations against *S. aureus*. The results show that antimicrobial activity of HAc is dependent on its concentrations. In the range of concentrations changing from 50 to 150 ppm, CFU ratios are not obviously different among the experimental groups. The results show that HAc at these concentrations exhibits slightly antimicrobial activities against *S. aureus*. When the concentration of HAc reaches 200 ppm, the CFU ratio is lower than those with low concentrations. HAc shows obvious antibacterial activities when its concentration is set as 300 ppm. Once the concentration is higher than 400 ppm, HAc can inhibit all *S. aureus*.

Antimicrobial activities of HAc with different concentrations against *E. coli* are shown in Fig. 7(b). At the concentrations ranging from 300 to 500 ppm, *E. coli* has been completely inhibited. When concentrations are changed from 150 to 200 ppm, HAc has no obvious effect on the growth of *E. coli*. The growth of *E. coli* is slightly promoted when the concentration of HAc varies from 50

Table 2
Parameters of thermal degradation of chitosan and chitosan-*N*-arginine (CS-*N*-Arg) samples.

Samples	First stage			Second stage		
	Range (°C)	T_{max1}	Weight loss (%)	Range (°C)	T_{max2}	Weight loss (%)
Chitosan	30–150	100.3	6.4	230–400	307.6	39.3
CS-*N*-Arg-1	30–120	65.3	3.8	200–280	266.5	30.5
CS-*N*-Arg-2	30–120	61.2	4.8	200–280	264.0	32.9
CS-*N*-Arg-3	30–120	55.0	6.5	200–280	258.4	33.0

to 100 ppm. Our results are well in agreement with the published report that *E. coli* will be completely inhibited when the concentrations of HAc are higher than 200 ppm due to the strong inhibitory effect (Liu et al., 2006). At the concentrations of HAc ranging from 150 to 200 ppm, the possibly promotional and inhibitory effects of HAc reach a level so that two effects could be balanced out. Thus, the numbers of tested groups and control become almost similar. At the concentrations changing from 50 to 100 ppm, HAc promotes the growth of *E. coli* possibly due to the reason that promotional effect of HAc is slightly stronger than its inhibitory effect.

3.3.2. *Effect of concentrations on the antibacterial activity of chitosan and CS-N-Arg*

The concentration-dependent antimicrobial activity of chitosan and CS-*N*-Arg samples against *S. aureus* is shown in Fig. 8(a). When the concentrations are higher than 150 ppm, the samples exhibit efficacious antibacterial activities and inhibit all of *S. aureus*. At a concentration of 100 ppm, the growth of *S. aureus* is significantly promoted as the DSs of arginine increased. At a concentration of 50 ppm, the bacteria-promoting ability of chitosan and CS-*N*-Arg samples is weakened.

The effect of concentrations on the antibacterial activity of chitosan and CS-*N*-Arg samples against *E. coli* is shown in Fig. 8(b). The results show that the higher DS of the CS-*N*-Arg specimens, the better antimicrobial ability. At a very low concentration of 50 ppm, chitosan and CS-*N*-Arg samples have some bacteria-promoting activities. This result is similar to some reports in which chitosan and its derivatives are found to promote the growth of *E. coli* at a low concentration (Liu et al., 2006). At a concentration of 100 ppm, CS-*N*-Arg-2 and CS-*N*-Arg-3 show antimicrobial properties, while chitosan and CS-*N*-Arg-1 still exhibit promotional effect of the growth of bacteria. At a concentration of 150 ppm, all samples show effective suppression against bacteria, and in particular, CS-*N*-Arg-2 and CS-*N*-Arg-3 can inhibit all the bacteria. When the concentration is higher than 200 ppm, the antibacterial activities of all of the four kinds of samples are almost the same, and all bacteria have been inhibited.

Antibacterial effect of CS-*N*-Arg on *S. aureus* is different from that on *E. coli*, which may be ascribed to their different cell wall structures or components. In Gram-positive bacteria, the cell wall is composed of a broad dense wall that is consisted of 15–40 interconnecting layers of peptidoglycans. At the concentrations higher than 150 ppm, positively charged free $-NH_3^+$ or/and guanidine groups of chitosan and CS-*N*-Arg can bind tightly to the components of cell walls, resulting in pore formation in cell walls, severe leakage of cell constituents and eventually the cell death (Kumar, Varadaraj, Gowda, & Tharanathan, 2005). When concentrations of chitosan and CS-*N*-Arg decrease, they are not able to destroy the cell walls in the form of distortion–disruption, and instead, chitosan and CS-*N*-Arg would be digested and adsorbed by bacteria as nutrition to accelerate the growth of the microbes. In addition, a result similar to previous report was also observed in our experiments, namely, it is found that chitosan derivatives with more positive charges show decreasing antibacterial activity against *S. aureus* (Holappa et al., 2006). These results may imply that the higher cationic charge is not responsible for better antimicrobial activity than that of unmodified chitosan.

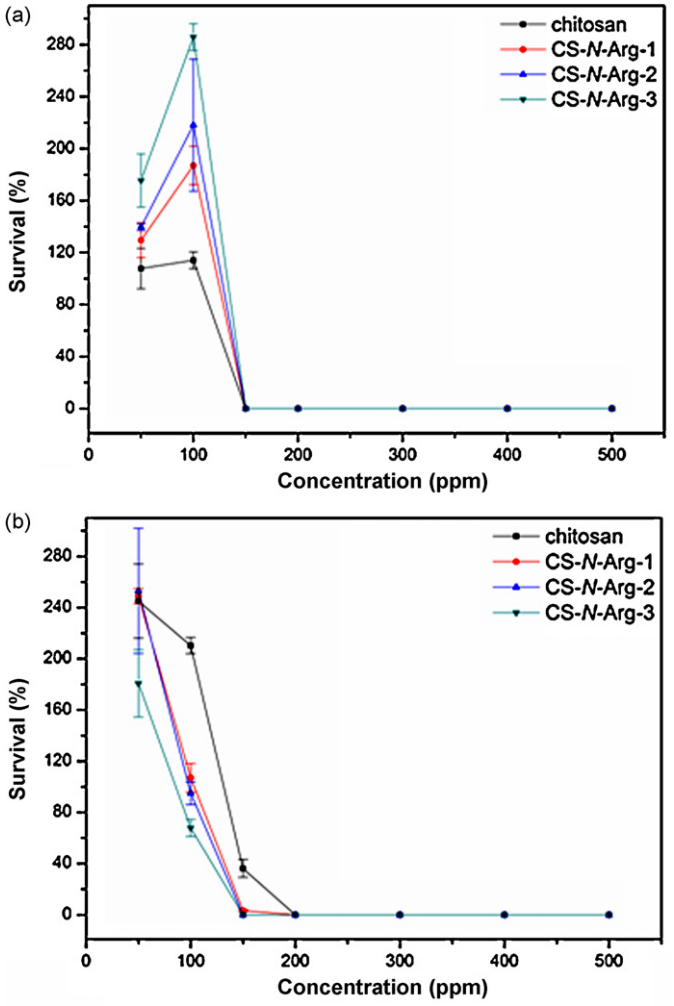

Fig. 8. Antibacterial activity of chitosan and chitosan-*N*-arginine (CS-*N*-Arg) samples on *S. aureus* (a) and *E. coli* (b). *S. aureus* and *E. coli* cells were spread onto culture medium agar plates with different concentrations of samples and incubated at 37 °C for 24 h. Data are mean ± standard deviation of quadruplicate.

The outer membrane of Gram-negative bacteria is normally built by a lipid bilayer with a thickness of about 7 nm, wherein lipopolysaccharide (LPS) and proteins are held together by electrostatic interactions with bivalent metal ions. When the concentration of chitosan and CS-*N*-Arg is over 200 ppm, the amino groups of chitosan or amino and guanidine groups in CS-*N*-Arg are bonded with the negatively charged *O*-specific antigenic oligosaccharide-repeating units of LPS, thus forming a compact layer around the cells, preventing the exchange of nutrients and metabolite wastes and destabilizing the cell walls (Liu, Du, Yang, & Zhu, 2004). In addition, due to the chelating ability of chitosan and its derivatives, the bivalent metal ions linked to LPS and proteins

form chelates with chitosan or CS-*N*-Arg. Based on this kind of interactions, cell walls of bacteria will become more volatile, leading to the leakage of cytoplasm constituents and resulting in the death of bacteria. At low concentrations, the samples are possibly assimilated into *E. coli* as food materials so as to promote the growth of cells.

There may be another antimicrobial mechanism in both *S. aureus* and *E. coli*. When the cell walls of bacteria are destabilized by chitosan or CS-*N*-Arg, the samples get through cell walls via porous or deformed zone by pervasion effect. As a result, chitosan and CS-*N*-Arg will combine with DNA, negative-charged enzymes and other functional factors in the cells to disturb the physiological activities of bacteria (Liu, Guan, Yang, Li, & Yao, 2001).

4. Conclusion

In the present study, chitosan derivatives with different degrees of substitution were successfully prepared. They showed significant pH-dependent solubility, and the degrees of substitution of arginine could be changed from 8.7 to 28.4% under the various reaction periods from 12 to 48 h. Some results showed that all CS-*N*-Arg specimens had a more amorphous structure than that of chitosan and their thermal stability was slightly lower compared to that of chitosan. CS-*N*-Arg samples exhibited obviously antibacterial activity against *S. aureus* and *E. coli* at the concentrations higher than 150 ppm. But at the concentrations lower than 50 ppm, they might be digested by microbes and absorbed as nutrients to promote the growth of microorganisms. These results also suggested that some optimized concentrations for CS-*N*-Arg and chitosan should be selected when they were used to control, suppress or completely inhibit the growth of bacteria.

Acknowledgements

This work was supported by the National Natural Science Foundation of China (contract grant numbers: 30870624; 30570493) and the National High-Technology Research and Development Project ("863" project) of China (contract grant numbers: 2006AA03Z439; 2007AA021901). We are also grateful to Prof. Shenqi Wang and Associate Prof. Lei Zhou for their contribution to the preparation of this manuscript.

References

Allan, G. G., & Peyron, M. (1995). Molecular weight manipulation of chitosan I: Kinetics of depolymerization by nitrous acid. *Carbohydrate Research*, *277*, 257–272.

An, N. T., Thien, D. T., Dong, N. T., & Dung, P. L. (2009). Water-soluble *N*-carboxymethylchitosan derivatives: Preparation, characteristics and its application. *Carbohydrate Polymers*, *75*, 489–497.

Arvanitoyannis, I. S. (1999). Totally and partially biodegradable polymer blends based on natural and synthetic macromolecules: Preparation, physical properties, and potential as food packaging materials. *Polymer Reviews*, *39*, 205–271.

Arvanitoyannis, I. S., Kolokuris, I., Nakayama, A., Yamamoto, N., & Aiba, S. (1997). Physico-chemical studies of chitosan-poly(vinyl alcohol) blends plasticized with sorbitol and sucrose. *Carbohydrate Polymers*, *34*, 9–19.

Badawy, M. E. I., & Rabea, E. I. (2009). Potential of the biopolymer chitosan with different molecular weights to control postharvest gray mold of tomato fruit. *Postharvest Biology and Technology*, *51*, 110–117.

Baker, T. J., Luedtke, N. W., Tor, Y., & Goodman, M. (2000). Synthesis and anti-HIV activity of guanidinoglycosides. *Journal of Organic Chemistry*, *65*, 9054–9058.

Chiang, Y. W., Wang, T. H., & Lee, W. C. (2009). Chitosan coating for the protection of amino acids that were entrapped within hydrogenated fat. *Food Hydrocolloids*, *23*, 1057–1061.

Chung, T. W., Yang, J., Akaike, T., Cho, K. Y., Nah, J. W., Kim, S. I., et al. (2002). Preparation of alginate/galactosylated chitosan scaffold for hepatocyte attachment. *Biomaterials*, *23*, 2827–2834.

El-Azzami, L. A., & Grulke, E. A. (2009). Carbon dioxide separation from hydrogen and nitrogen facilitated transport in arginine salt-chitosan membranes. *Journal of Membrane Science*, *328*, 15–22.

Gil, G., del Mónaco, S., Cerrutti, P., & Galvagno, M. (2004). Selective antimicrobial activity of chitosan on beer spoilage bacteria and brewing yeasts. *Biotechnology Letters*, *26*, 567–574.

Gobbi, A., & Frenking, G. (1993). Y-conjugated compounds: The equilibrium geometries and electronic structures of guanidine, guanidine cation, urea, and 1,1-diaminoethylene. *Journal of the American Chemistry Society*, *115*, 2362–2372.

Guan, Y., Xiao, H. N., Sullivan, H., & Zheng, A. N. (2007). Antimicrobial-modified sulfite pulps prepared by in situ copolymerization. *Carbohydrate Polymers*, *69*, 688–696.

Holappa, J., Hjálmarsdóttir, M., Másson, M., Rúnarsson, Ö., Asplund, T., Soininen, P., et al. (2006). Antimicrobial activity of chitosan *N*-betainates. *Carbohydrate Polymers*, *65*, 114–118.

Jintapattanakit, A., Mao, S. R., Kissel, T., & Junyaprasert, V. B. (2008). Physicochemical properties and biocompatibility of *N*-trimethyl chitosan: Effect of quaternization and dimethylation. *European Journal of Pharmaceutics and Biopharmaceutics*, *70*, 563–571.

Kitagaki, H., Araki, Y., Funato, K., & Shimoi, H. (2007). Ethanol-induced death in yeast exhibits features of apoptosis mediated by mitochondrial fission pathway. *FEBS Letters*, *581*, 2935–2942.

Kumar, A. B. V., Varadaraj, M. C., Gowda, L. R., & Tharanathan, R. N. (2005). Characterization of chitooligosaccharides prepared by chitosanolysis with the aid of papain and pronase, and their bactericidal action against *Bacillus cereus* and *Escherichia coli*. *Biochemical Journal*, *391*, 167–175.

Kumirska, J., Weinhold, M. X., Sauvageau, J. C. M., Thöming, J., Kaczyński, Z., & Stepnowski, P. (2009). Determination of the pattern of acetylation of low-molecular-weight chitosan used in biomedical applications. *Journal of Pharmaceutical and Biomedical Analysis*, *50*, 587–590.

Lavertu, M., Méthot, S., Tran-Khanh, N., & Buschmann, M. D. (2006). High efficiency gene transfer using chitosan/DNA nanoparticles with specific combination of molecular weight and degree of deacetylation. *Biomaterials*, *27*, 4815–4824.

Liu, H., Du, Y. M., Yang, J. H., & Zhu, H. Y. (2004). Structural characterization and antimicrobial activity of chitosan/betain derivative complex. *Carbohydrate Polymers*, *55*, 291–297.

Liu, N., Chen, X. G., Park, H. J., Liu, C. G., Liu, C. S., Meng, X. H., et al. (2006). Effect of MW and concentration of chitosan on antibacterial activity of *Escherichia coli*. *Carbohydrate Polymers*, *64*, 60–65.

Liu, W. G., Zhang, J. R., Cao, Z. Q., Xu, F. Y., & Yao, K. D. (2004). A chitosan–arginine conjugate as a novel anticoagulation biomaterial. *Journal of Materials Science: Materials in Medicine*, *15*, 1199–1203.

Liu, X. F., Guan, Y. L., Yang, D. Z., Li, Z., & Yao, K. D. (2001). Antimicrobial action of chitosan and carboxymethylated chitosan. *Journal of Applied Polymer Science*, *29*, 1324–1335.

Lu, Z. S., Li, C. M., Bao, H. F., Qiao, Y., Hoh, Y. H., & Yang, X. (2008). Mechanism of antimicrobial activity of CdTe quantum dots. *Langmuir*, *24*, 5445–5452.

Mima, S., Miya, M., Iwamoto, R., & Yoshikawa, S. (2003). Highly deacetylated chitosan and its properties. *Journal of Applied Polymer Science*, *28*, 1909–1917.

Qin, C. Q., Xiao, Q., Li, H. R., Fang, M., Liu, Y., Chen, X. Y., et al. (2004). Calorimetric studies of the action of chitosan-*N*-2-hydroxypropyltrimethyl ammonium chloride on the growth of microorganisms. *International Journal of Biological Macromolecules*, *34*, 121–126.

Sadeghi, A. M. M., Dorkoosh, F. A., Avadi, M. R., Saadat, P., Rafiee-Tehrani, M., & Junginger, H. E. (2008). Preparation, characterization and antibacterial activitie of chitosan, *N*-trimethyl chitosan (TMC) and *N*-diethylmethyl chitosan (DEMC) nanoparticles loaded with insulin using both the ionotropic gelatin and polyelectrolyte complexation methods. *International Journal of Pharmaceutics*, *355*, 299–306.

Yao, X. S. (1994). *Natural medicine chemistry*. Beijing: People's Medical Publication House. (in Chinese).

Zhang, Y. M., Jiang, J. M., & Chen, Y. M. (1999). Synthesis and antimicrobial activity of polymeric guanidine and biguanidine salts. *Polymer*, *40*, 6189–6198.

Zhang, Y. Q., Xue, C. H., Xue, Y., Gao, R. C., & Zhang, X. L. (2005). Determination of the degree of deacetylation of chitin and chitosan by X-ray powder diffraction. *Carbohydrate Research*, *340*, 1914–1917.

Zhong, Z. M., Xing, R., Liu, S., Wang, L., Cai, S. B., & Li, P. C. (2008). Synthesis of acyl thiourea derivatives of chitosan and their antimicrobial activities in vitro. *Carbohydrate Research*, *343*, 566–570.

Zhu, D. W., Zhang, H. L., Bai, J. G., Liu, W. G., Leng, X. G., Song, C. X., et al. (2007). Enhancement of transfection efficiency for Hela cells via incorporating arginine moiety into chitosan. *Chinese Science Bulletin*, *52*, 3207–3215.

Zhu, J. H., Wang, X. W., Ng, S., Quek, C. H., Ho, H. T., Lao, X. J., et al. (2005). Encapsulating live cells with water-soluble chitosan in physiological conditions. *Journal of Biotechnology*, *117*, 355–365.